particles

IMPACT FACTOR 2.3

CITESCORE 3.0

Article

POEMMA–Balloon with Radio: A Balloon-Borne Multi- Messenger Multi-Detector Observatory

Giuseppe Osteria, Johannes Eser and Angela Olinto

Special Issue

Advances in Space AstroParticle Physics: Frontier Technologies for Particle Measurements in Space, 2025 Edition

Edited by

Dr. Matteo Duranti and Dr. Valerio Vagelli

MDPI

https://doi.org/10.3390/particles9010019

particles

MDPI

Article

POEMMA–Balloon with Radio: A Balloon-Borne Multi-Messenger Multi-Detector Observatory

Giuseppe Osteria [1,*], Johannes Eser [2] and Angela Olinto [2] on behalf of the JEM-EUSO Collaboration

[1] Istituto Nazionale di Fisica Nucleare—Sezione di Napoli, 80126 Naples, Italy
[2] Columbia Astrophysics Laboratory, Columbia University, New York, NY 10027, USA; jbe2130@columbia.edu (J.E.)
* Correspondence: giuseppe.osteria@na.infn.it

Abstract

The Probe Of Extreme Multi-Messenger Astrophysics (POEMMA) is a proposed dual-satellite mission to observe Ultra-High-Energy Cosmic Rays (UHECRs), increase the statistics at the highest energies, and observe Very-High-Energy Neutrinos (VHENs) following multi-messenger alerts of astrophysical transient events, such as gamma-ray bursts and gravitational wave events, throughout the universe. POEMMA–Balloon with radio (PBR) is a small-scale version of the POEMMA design, adapted to be flown as a payload on one of NASA's suborbital Super Pressure Balloons (SPBs) circling over the Southern Ocean for more than 20 days after a launch from Wanaka, New Zealand. The main science objectives of PBR are: (1) to observe UHECRs via the fluorescence technique from suborbital space; (2) to observe horizontal high-altitude air showers (HAHAs) with energies above the cosmic ray knee (E > 3PeV) using optical and radio detection for the first time; and (3) to follow astrophysical event alerts in the search of VHENs. The PBR instrument consists of a 1.1 m aperture Schmidt telescope similar to the POEMMA design, with two cameras on its focal surface: a Fluorescence Camera (FC) and a Cherenkov Camera (CC). In addition, PBR has a Radio Instrument (RI) optimized for detecting EASs (covering the 60–660 Mhz range). The FC observes UHECR-induced EASs in the ultraviolet (UV) spectrum using an array of 9216-pixel Multi-Anode Photo-Multiplier Tubes (MAPMTs) imaged every 1 μs. The CC uses a 2048-pixel Silicon Photo-Multiplier (SiPM) imager to observe cosmic-ray-induced HAHAs and search for neutrino-induced upward-going EASs. The CC covers a spectral range of 320–900 nm, with an integration time of 10 ns. This contribution provides an overview of PBR instruments and their current status.

Keywords: ultra-high-energy cosmic rays; very-high-energy neutrinos; fluorescence camera; Cherenkov camera; radio instrument

Academic Editors: Matteo Duranti, Valerio Vagelli and Armen Sedrakian

Received: 1 December 2025
Revised: 6 January 2026
Accepted: 6 February 2026
Published: 16 February 2026

1. Introduction

Over recent decades, research on Ultra-High-Energy Cosmic Rays (UHECRs, E > 1 EeV) and Very-High-Energy Neutrinos (VHENs, E > 1 PeV) has advanced considerably thanks to today's largest ground-based observatories: the Pierre Auger Observatory (Auger) [1] in the Southern Hemisphere, the Telescope Array (TA) [2] in the Northern Hemisphere and the IceCube Neutrino Observatory (IceCube) [3] in Antartica. The energy spectra and mass compositions of UHECRs have been determined with notable precision thanks to Auger and TA. These facilities have also revealed early indications of anisotropies in the arrival directions of these particles [4]. Nevertheless, key issues remain unresolved, such as the

cosmological evolution of their sources and the physical mechanisms responsible for their production and acceleration. The consensus among the scientific community is that two complementary classes of next-generation detectors are essential to obtain the necessary data: (1) instruments offering high-precision measurements and (2) detectors providing maximal exposure at the highest energies [5].

Beyond upgrades to existing instruments, such as AugerPrime, the Pierre Auger Observatory [6], and TA×4, and the extension of TA [7], IceCube-Gen2, and the IceCube Neutrino Observatory [8], a step forward for high-precision measurements will be the proposed Global Cosmic Ray Observatory (GCOS) [9], which will combine an order-of-magnitude higher exposure than current ground arrays with high measurement accuracy provided by combining several detection techniques. The highest exposures will be provided by observations from the ground with cosmic ray measurements of the Giant Radio Array for Neutrino Detection (GRAND) [10] and from space with the proposed dual-satellite project Probe for Multi-Messenger Astrophysics (POEMMA) [11] or the more recent M-EUSO concept [12]. Such instruments are perhaps the only ones capable of looking for ZeV particles and a recovery in the flux beyond the suppression. Furthermore, the observations from space allow for obtaining very large exposure along with full-sky observation. Space-based missions would detect neutrinos by capturing the Cherenkov emission generated by upward-going extensive air showers (EASs). Such showers occur when a charged lepton—produced after a neutrino crosses the Earth and interacts near its surface—decays in the atmosphere. UHECRs, on the other hand, would be observed via the fluorescence light produced by EASs triggered by the interactions of primary cosmic rays with atmospheric nuclei. Stratospheric balloon campaigns represent an ideal intermediate stage on the path to a satellite mission. They allow researchers to enhance technological readiness levels, validate detection strategies, and gather initial scientific data—all with reduced risk, shorter timelines, and lower cost compared to a full space-based observatory. The POEMMA–Balloon with Radio (PBR) project is currently the most advanced stratospheric balloon initiative led by the JEM-EUSO collaboration. It incorporates a hybrid focal surface within a wide-field Schmidt telescope inspired by the POEMMA design and builds upon the achievements of previous balloon flights, including EUSO-SPB1 [13] and EUSO-SPB2 [14]. Despite difficulties related to balloon stability, these earlier missions yielded crucial technical experience and demonstrated the viability of the approaches now implemented in PBR.

2. PBR Mission

The PBR mission is planned to launch aboard a NASA Super Pressure Balloon (SPB) from Wanaka, New Zealand, during the first half of 2027. The balloon is expected to remain aloft for over 20 days. Throughout the mission, the payload will drift above the Southern Ocean, monitoring the atmosphere below and collecting nighttime observations from an altitude of roughly 33 km.

The main elements of the PBR payload (Figure 1) include a large tiltable telescope equipped with a hybrid focal surface, as well as a Radio Instrument (RI) made up of two antennas positioned beneath the telescope. Completing the instrument suite are a compact X-gamma detector and an infrared (IR) camera, which will track cloud coverage both inside and around the primary field of view.

The telescope (Figure 2) adopts a modified Schmidt configuration featuring a 1.1 m entrance aperture, which is fitted with an aspheric PMMA corrector plate to eliminate spherical aberrations. The primary mirror consists of 12 segmented elements and has a radius of curvature of 1.6 m. This optical setup yields an expected point-spread function with 95% of the light contained within a 3 mm diameter spot and provides a field of view of about $36^\circ \times 36^\circ$ at the focal plane. Situated at the focal surface is the hybrid

camera, composed of two subsystems: the fluorescence camera (FC), tailored for UHECR observations using the fluorescence method, and the Cherenkov camera (CC), intended to detect Cherenkov emission from Earth-skimming neutrinos or from high-altitude, nearly horizontal air showers. The design and performance of both instruments are presented in the following sections.

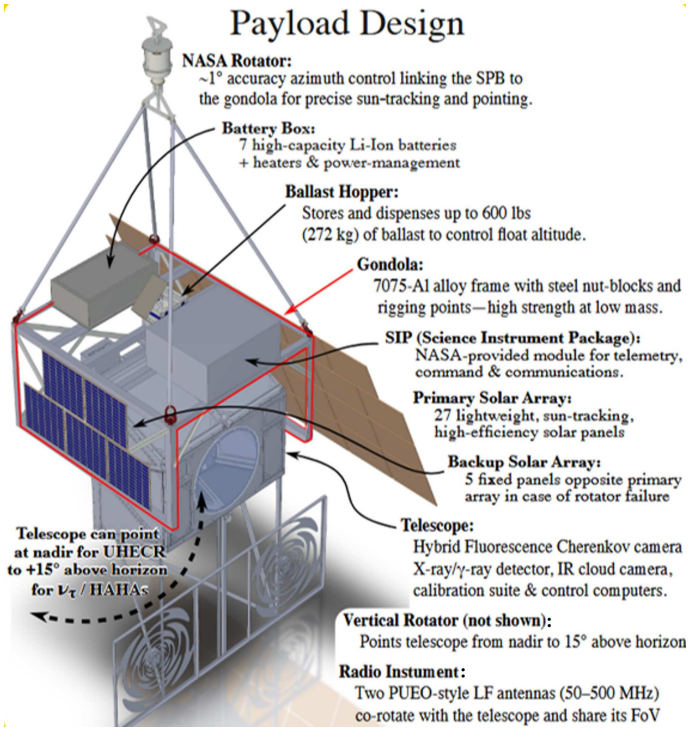

Figure 1. Design of the full PBR payload, including SPB equipment [15].

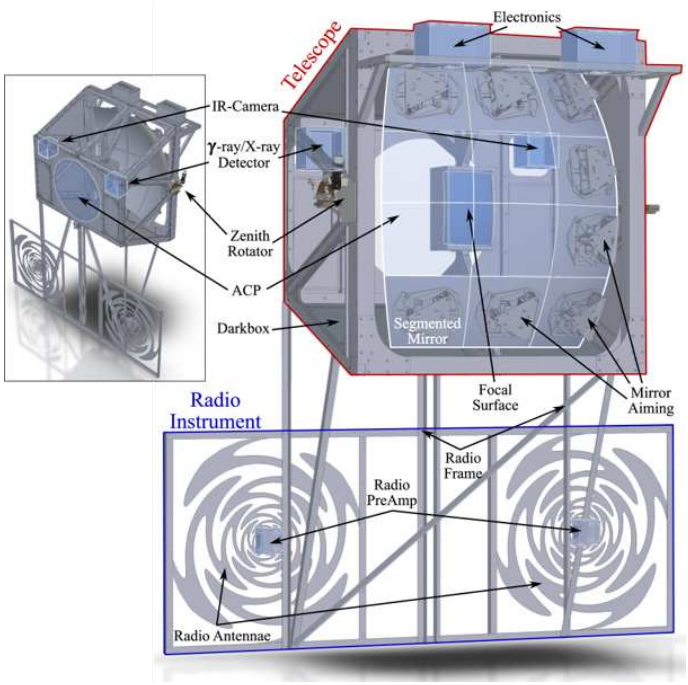

Figure 2. Detailed design drawing of the two main PBR detectors: the Schmidt telescope with its hybrid focal surface and the radio antennas mounted beneath [15].

https://doi.org/10.3390/particles9010019

2.1. Fluorescence Camera

The Fluorescence Camera adopted for PBR [16] builds upon the Hamamatsu 64-channel multianode photomultiplier tube (MAPMT) (model R11265-203-M64) improved from that used in previous missions. Four 64-channel MAPMTs form an elementary cell, and nine such cells constitute a Photo Detection Module (PDM), yielding 2304 pixels per module. With four PDMs (Figure 3) installed on PBR, the FC provides a total of 9216 pixels arranged on the integrated focal surface shared with the Cherenkov Camera, following the architecture demonstrated in EUSO-SPB2. Signal readout is managed through the Spaciroc3 ASIC, which supports single-photoelectron counting with a 1 µs integration time and a double-pulse resolution of approximately 10 ns. These performance characteristics make the FC well-suited for reconstructing the ultraviolet fluorescence signatures produced by Extensive Air Showers (EASs) initiated by Ultra-High-Energy Cosmic Rays (UHECRs). To suppress background illumination and preserve sensitivity to nitrogen fluorescence, a BG3 optical filter limits the detection band to 290–430 nm. Mounted on the focal surface of the 1.1 m Schmidt telescope specifically optimized for a super-pressure balloon platform, the four PDMs provide a combined field of view (FoV) of roughly $24^\circ \times 24^\circ$, with an instantaneous FoV of $0.2^\circ \times 0.2^\circ$ per pixel. This expansion in FoV (about 25% larger than in EUSO-SPB2) and the increased aperture are expected to significantly enhance the event rate and lower the energy threshold for UHECR fluorescence detection. Simulations presented in the PBR design study indicate that a non-negligible fraction of recorded tracks will be sufficiently long to enable reconstruction of the full longitudinal shower profile, including the shower maximum X_{max}, thereby supporting energy, directional, and composition analyses. The FC also benefits from the telescope's capability to continuously tilt between nadir and near-horizontal orientations, a strategy intended to maximize exposure to UHECRs at the highest energies. This scanning flexibility—tested for the first time in flight within PBR—allows the mission to evaluate operational modes envisioned for future space-based observatories such as the POEMMA.

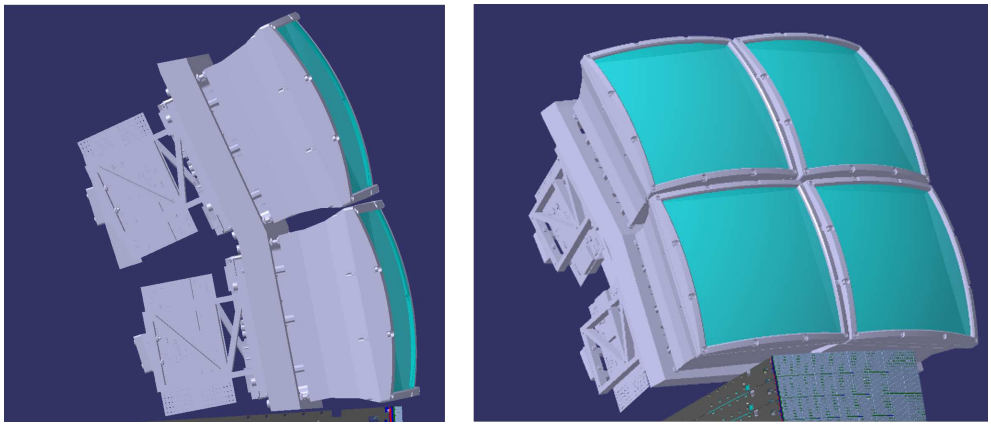

Figure 3. CAD rendering of the Fluorescence Camera. (**Left**): Side view of the camera. (**Right**): Front view of the four PDMs of the camera.

2.2. Cherenkov Camera

The 2048-pixel CC [17] has a modular design comprising four PDMs, each consisting of eight SiPM arrays (see Figure 4). The total field of view spans $12^\circ \times 6^\circ$, with each pixel subtending 0.2°. To reduce noise triggers, a bi-focalizing optical system—requiring local and temporal coincidence—is being developed for installation in front of the camera.

The current baseline choice for the 8×8 SiPM arrays is the Hamamatsu S13361-3050 model, sensitive to wavelengths in the range 320–900 nm, selected for its low afterpulse and crosstalk probabilities, high PDE in the UV range, and established radiation tolerance. Each

SiPM has an effective photosensitive area of 3×3 mm^2 and a 50 µm pitch. To optimize optical performance, the arrays are mounted on a curved support structure approximating the spherical curvature of the telescope's focal surface. The curved structure is designed to minimize dead space while keeping connections to the readout electronics flexible. The connection between the sensor and the electronics is made by micro coaxial cables (by the Samtec company). This ensures optimized use of the space on the back of the SiPM matrix and allows mounting the sensors with minimal clearance between them. The readout electronics will be based on next-generation ASICs optimized for low power consumption and advanced functionality. The main candidate is the 64-channel CMOS MIZAR ASIC [18] (developed by the INFN in Turin, Italy), which integrates a front-end amplifier, 256 memory cells sampling at 200 MHz, and a programmable ADC with a 7–12 bit resolution. Each channel consumes about 10 mW, and the bi-focal optical design requires coincidence of at least two pixels to generate a trigger, reducing false positives. An alternative solution, albeit with lower performance but already commercially available, is a Radioroc2 ASIC produced by Weeroc. While this option does not allow for wavelength digitization, it offers a lower data budget solution. The use of Radioroc2 ASIC allows for channel-by-channel adjustment of high-voltage SiPMs [19], enabling fine SiPM gain adjustment to correct for channel gain non-uniformity. Additionally, this ASIC can trigger at levels as low as 1/3 photoelectron, offering dual-gain energy measurement capabilities, and maintains 1% linearity in energy measurement up to 2000 photoelectrons. A board (ASIC board) hosting eight MIZAR or Radioroc2 ASICs, guarantees the readout of the 512 pixels of a PDM. A second board (FPGA board) provides control functionalities, implements the second-level trigger logic, and performs data acquisition from the ASICs. Both ASIC boards are compatible with the same control FPGA board.

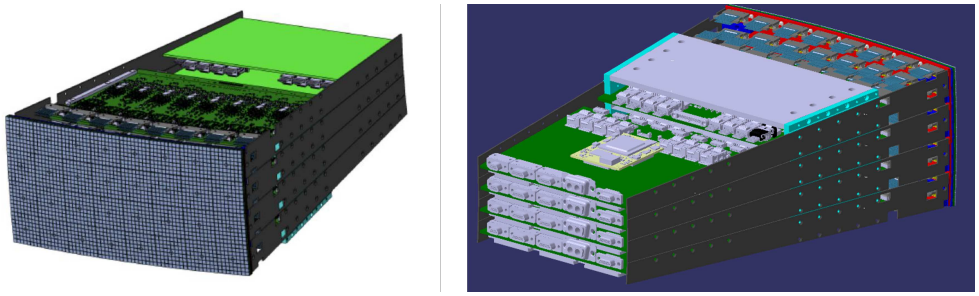

Figure 4. CAD rendering of the Cherenkov Camera. (**Left**) Front view with the SiPM sensors of the curved focal surface in the foreground. (**Right**) Rear view: the readout electronics and the cooling plate are better visible in this view.

2.3. Radio Instrument

PBR's Radio Instrument (RI) is composed of two dual-polarized sinuous antennas derived from the Low Frequency (LF) subsystem developed for PUEO and adapted for enhanced sensitivity to radio emission from extensive air showers [20]. The antennas are scaled to 52-inch apertures, providing a broadband response of approximately 5 dBi over the 60–660 MHz range. They are installed one meter apart and oriented in the same direction to enable coherent beamforming, which yields an effective gain of about 6.5 dBi. This configuration not only enhances signal-to-noise performance but also permits azimuthal reconstruction of the radio pulses and secures a field of view of roughly $\pm 30^\circ$. Each antenna is fabricated from copper to improve broadband efficiency and is patterned on an FR4 substrate. The substrate is bonded to an aramid honeycomb core with an FR4 backplate, which provides mechanical rigidity while also supporting the mounting of front-end electronics. The RI is positioned directly beneath PBR's optical payload (see Figure 2) and aligned with the telescope's optical axis, ensuring that the radio and optical instruments

share overlapping fields of view during zenith and azimuth scans. This arrangement is central to PBR's hybrid-detection strategy, which aims to combine radio and Cherenkov measurements to reconstruct air shower geometry and energy with improved accuracy. The RI primarily operates in an externally triggered mode, in which triggers generated by the Cherenkov Camera (CC) initiate radio waveform acquisition. This allows for hybrid observation of air showers and leverages the CC's higher instantaneous sensitivity to initiate coincident measurements. In addition, the RI includes a dedicated radio-only self-trigger path designed for periods when the CC is offline—particularly during daytime operations—and optimized to capture high-signal-amplitude, atmosphere-skimming showers. Supporting this capability is a waveform-sampling back-end based on a DRS4 ASIC, enabling nanosecond-scale digitization of radio pulses for detailed reconstruction of the temporal and spectral structure of the signals. Development of the RI's optimized electronics is currently ongoing, building directly upon the extensive testing performed for the PUEO LF system. According to the current project schedule, the first hardware prototypes are expected to undergo laboratory testing in the coming months, followed by integrated system tests with PBR's optical subsystems. Complementary simulation studies are also underway to quantify the standalone sensitivity of the RI to nearly horizontal air showers and to evaluate its contribution to PBR's overall exposure to Ultra-High-Energy Cosmic Rays.

2.4. The X-γ Instrument

The PBR X-γ instrument is designed to explore the possibility of detecting X-rays and gamma rays generated via synchrotron radiation, in the early stage of the HAHA's EAS development, by high-energy electrons and positrons from its electromagnetic component [21]. The X-γ instrument can detect high-energy photons starting from energies of $\simeq$15 keV, thereby extending the mission's sensitivity into the soft X-ray and γ-ray domains.

Figure 5 presents an exploded view of the full detector assembly. The photon detection system is based on four commercial Scionix modules, each consisting of a NaI(Tl) or CsI(Tl) scintillating crystal coupled to a SiPM readout stage with an integrated preamplifier. The manufacturer provides each module with built-in bias-generation electronics and a temperature-compensation loop to stabilize the SiPM gain across the thermal variations expected during balloon flight. To cover the broad energy range of interest, three detector types are employed—an X Channel ($\geq$15 keV), an X–γ Channel ($\geq$20 keV), and two γ Channels ($\geq$50 keV)—each optimized for its target energy band. The X Channel incorporates a 0.3 mm beryllium entrance window to minimize absorption of low-energy photons, while the other channels use 0.1 mm aluminum windows appropriate for higher energies. All four detection units are mounted within a dedicated collimator assembly that restricts the field of view to 16° for the X Channel and 30° for the remaining channels. The detector assembly is surrounded by a plastic-scintillator anticoincidence system (shown in light blue in Figure 5), read out by four SiPMs, which serves as a veto for charged particles. To preserve low-energy throughput, the entrance aperture of the X Channel is intentionally excluded from the veto enclosure; instead, a permanent magnet embedded within the collimator is used to deflect incoming charged particles away from the soft-X-ray detector. This design choice minimizes passive material in front of the lowest-energy channel while retaining efficient background suppression. The overall configuration, mechanically supported by lightweight structures described in the PBR instrument design report, follows established strategies adopted in balloon-borne high-energy detectors. A single electronics board equipped with an embedded FPGA provides power distribution, control of module parameters, and implementation of the trigger logic. The FPGA manages the digitization

and readout of eight channels: four from the primary scintillation detectors and four from the plastic–scintillator veto. This compact and robust architecture enables reliable operation in the stratospheric environment and allows coordinated triggering with the other PBR instruments, contributing to the mission's multi-wavelength observational capability.

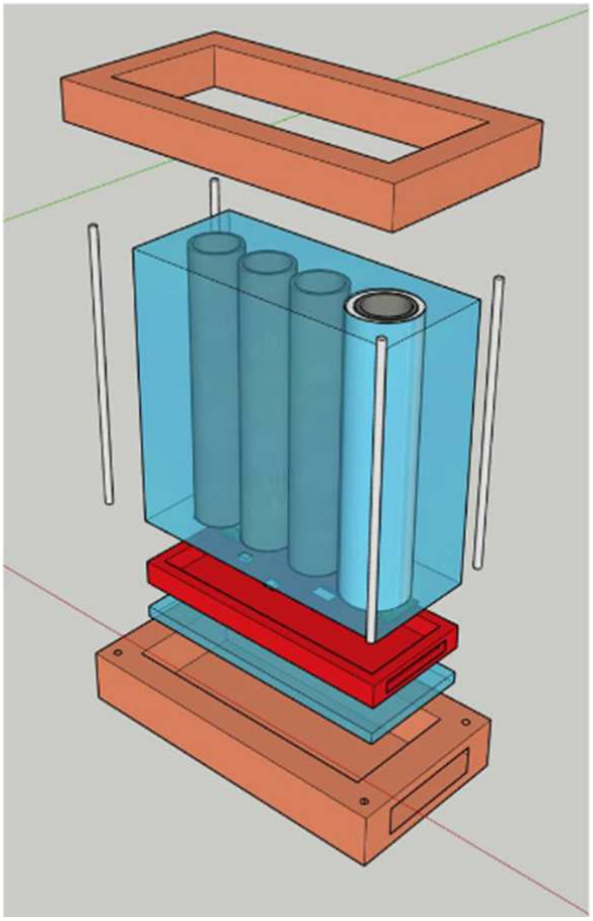

Figure 5. Cad rendering of the X-γ detector. The low-energy X-ray channel is the one on the right with the gray opening. The cyan-colored blocks represent the anti-coincidence system. The whole system is enclosed in a 2 mm aluminum box, not shown in the picture.

3. FC Expected Performances

Based on this instrument design and on the operational experience accumulated during previous balloon missions, an extensive simulation study has been performed using the EUSO–Offline framework [22] to evaluate the expected performance of the FC. The simulation methodology—originally developed for the EUSO-SPB1 and EUSO-SPB2 flights—follows the approach detailed in [23]. The EASs simulated in CONEX [24], using the EPOS LHC hadronic interaction model [25], are the precursor for the simulation. The profile of light, from fluorescence and Cherenkov emission, is calculated and propagated through the atmosphere, accounting for Mie and Rayleigh scattering. The photons that reach the telescope's aperture are then projected onto a simulated focal surface using parameters based on accurate laboratory measurements, also described in [23], followed by a detailed simulation of the electronics, including the trigger algorithm. The effective aperture of the FT is calculated by a method to account for all of the possible geometries of observable showers by an aerial detector looking down at the atmosphere. The method consists of simulating many showers, sampling an oversized area beneath the detector, and converting the fraction of events that trigger into a triggered aperture. Two million showers in total have been thrown over a 100 km radius disk covering all possible geometries in the

energy range from $10^{17.8}$ eV to $10^{19.7}$ eV. The triggered aperture at each energy is converted into an expected event rate via measurements of the UHECR energy spectrum reported by the Pierre Auger Observatory [26]. The method has been adapted to the enhanced optical throughput and expanded $24^\circ \times 24^\circ$ field of view of PBR's 1.1 m Schmidt telescope [16]. In particular, the ability of PBR to tilt between nadir and near-limb geometries, a key improvement relative to earlier missions, has been incorporated to quantify the impact on exposure and energy threshold. The results of this study, already presented in a previous work [15], are summarized in Figure 6. Two representative pointing configurations were studied. In the nadir geometry, where the telescope optical axis is directed vertically downward, the minimum detectable energy is $\simeq$1.8 EeV, yielding an event rate of approximately 0.28 EAS per hour of observation. When the instrument is oriented toward the Earth's limb—so that the top of the FC FoV is aligned with the atmospheric boundary—the geometric aperture increases substantially. However, the corresponding energy threshold rises to $\simeq$4 EeV due to the reduced fluorescence brightness at larger distances, resulting in a lower event rate of about 0.12 events per hour. The simulation results indicate that more than 10% of detected showers will meet the high-quality criteria adopted in [16], meaning that the recorded light profiles are sufficiently long and bright to enable reconstruction of the arrival direction, energy, and—for a subset of events—the depth of maximum development $X_{\max}$, which provides composition sensitivity. These findings confirm that PBR will achieve the first observation of extensive air showers from above using the fluorescence technique, thereby increasing the corresponding technology readiness level (TRL) to 6, in line with the requirements for future space-based UHECR missions.

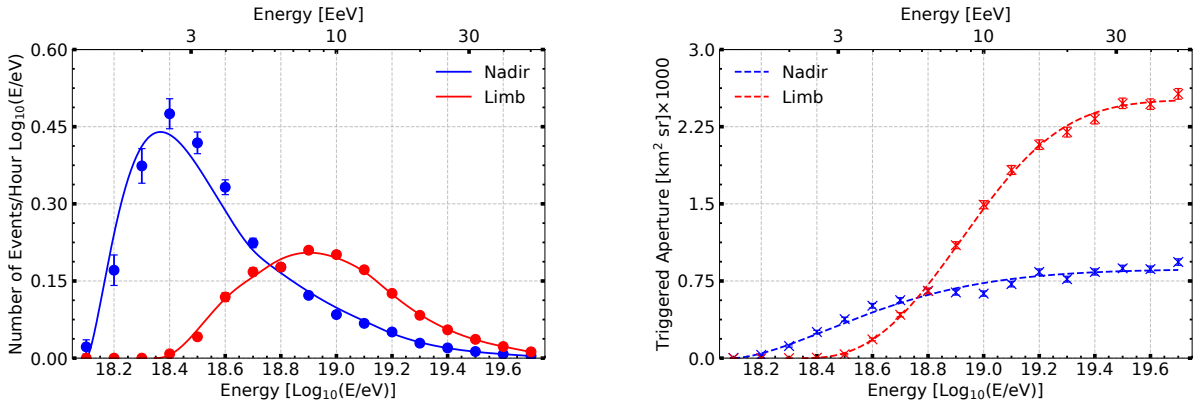

Figure 6. (**Left**): Preliminary event rate of PBR for two pointing scenarios—nadir (blue) and limb (red) [15]. (**Right**): Triggered aperture of PBR for both pointing scenarios [15].

CC Expected Performances

The CC design allows PBR to investigate High-Altitude Horizontal Air Showers (HAHAs) when the telescope is pointed above the limb, while orientations below the limb enable searches for astrophysical neutrinos via upward-going or skimming trajectories.

The study of High-Altitude Heavy Air Showers (HAHAs) is significant for two main reasons. First, High-Energy Cosmic Ray events ($\geq$PeV) exhibit fluxes that are four orders of magnitude higher than those of astrophysical neutrinos within the same energy spectrum. Second, the atmospheric refraction of optical Cherenkov emissions can cause signals from above the Earth's limb to appear as though they originate from below it, creating a false impression of neutrino-induced events. This phenomenon adds background noise to the detection of actual below-the-limb neutrino events. To assess the detection rate of HAHAs, a comprehensive simulation framework (EASCherSim) has been implemented to study the trajectories of above-the-limb cosmic rays, their Cherenkov emissions at PeV energies and higher, and how the geomagnetic field influences the Cherenkov signal in

a high-altitude, low-density atmosphere. The methods, with their relative assumptions, limitations, and uncertainties, are described in [27,28]. Some of the results of these studies, already presented in a previous work [15], are summarized in Figure 7. The left panel shows the sample trajectories. For a 20% operational duty cycle across a nominal 30-day super-pressure-balloon flight, the central panel of Figure 7 indicates an event rate of approximately 60 events per hour for an energy threshold of $\simeq$500 TeV. Because only very energetic horizontal showers can traverse a large angular extent within the CC field of view, a geometric-energy filter can be applied: high-energy events occupy a broad angular range, whereas lower-energy (and more frequent) events are confined to the upper portion of the CC focal plane. This purely geometric selection provides a first-order energy estimator without requiring full longitudinal profile reconstruction. PBR represents the first mission to combine such optical HAHA measurements with coincident radio observations from the instrument described in Section 2.3. The shared pointing geometry, enabled by the common Schmidt optical axis and co-aligned field of view, allows simultaneous Cherenkov and radio detection of the same events. This hybrid approach has the potential to improve event classification and may offer sensitivity to the primary composition of the cosmic rays producing HAHAs, thus extending the science reach of PBR beyond the capabilities of previous balloon-borne missions.

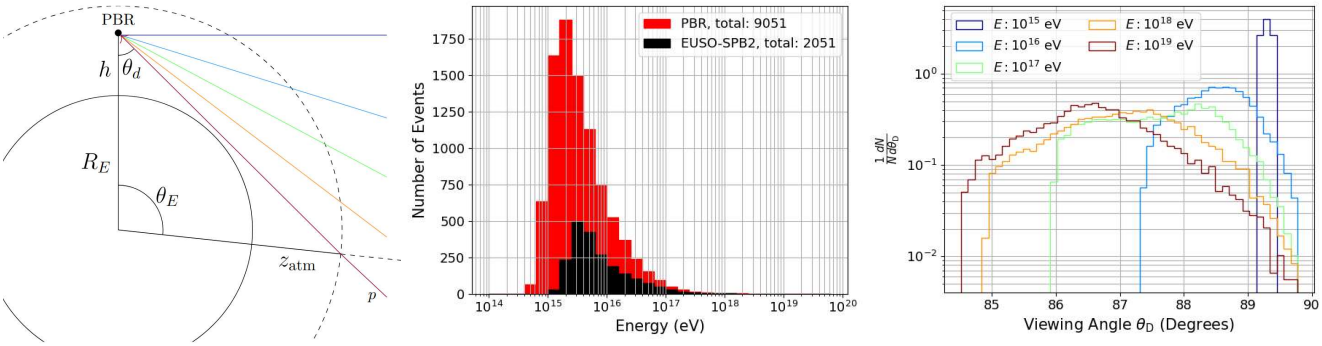

Figure 7. (**Left**): Example HAHA trajectories illustrating the large atmospheric distances traversed [15]. (**Center**): Expected event rate for a 30-day flight (red: PBR, black: EUSO-SPB2) [15]. (**Right**): Angular distribution for different primary cosmic ray energies [15].

When oriented below the Earth's limb, the CC and RI become sensitive to the Cherenkov emission produced by upward-going extensive air showers (EASs) initiated by Earth-skimming neutrinos, predominantly ν_τ, making PBR a pioneering platform for the study of astrophysical neutrino sources. In this geometry, the Earth acts as a neutrino converter: PeV–EeV ν_τ may interact within the crust to produce emerging τ-leptons that decay in flight and generate observable EASs, while ultra-relativistic muons from ν_μ interactions can also yield detectable Cherenkov signatures [29]. Such detections would provide insights into cosmic ray acceleration environments and hadronic interaction zones, contributing to the broader multi-messenger framework that includes photons and gravitational waves. Given the limited duration of the mission (even under optimistic 100-day scenarios) and the relatively narrow instantaneous field of view, PBR is not expected to achieve competitive limits on the diffuse cosmogenic neutrino flux, in agreement with current constraints from IceCube and Auger [27]. Instead, PBR's principal strength lies in its ability to rapidly repoint toward astrophysical events following external alerts, enabling time-critical Target-of-Opportunity (ToO) observations. This capability is central to PBR's science program [29,30], allowing searches for neutrinos from transient sources such as supernovae, binary neutron star mergers, tidal disruption events, blazar flares, and gamma-ray bursts. The CC's projected point-source sensitivity for ToO observations is

comparable to that of leading ground-based neutrino telescopes and, when combined with the RI, extends the accessible energy range well beyond the PeV scale, particularly above 300 PeV where radio detection becomes increasingly advantageous.

Figure 8, already presented in [15], shows the main results of the simulation studies. The left panel shows the resulting all-flavor 90% CL sensitivities for optimally timed 1000 s ToO exposures computed with the `νSpaceSim` package [31], along with comparison limits from IceCube, Auger, and ANTARES for the GW170817 event [32]. The right panel displays a sky map of the time-averaged effective area expected from a 100-day mission in April 2027, incorporating Sun and Moon avoidance constraints and the telescope's full tilting capabilities. A detailed description of the simulation framework and the sensitivity calculations is provided in [30].

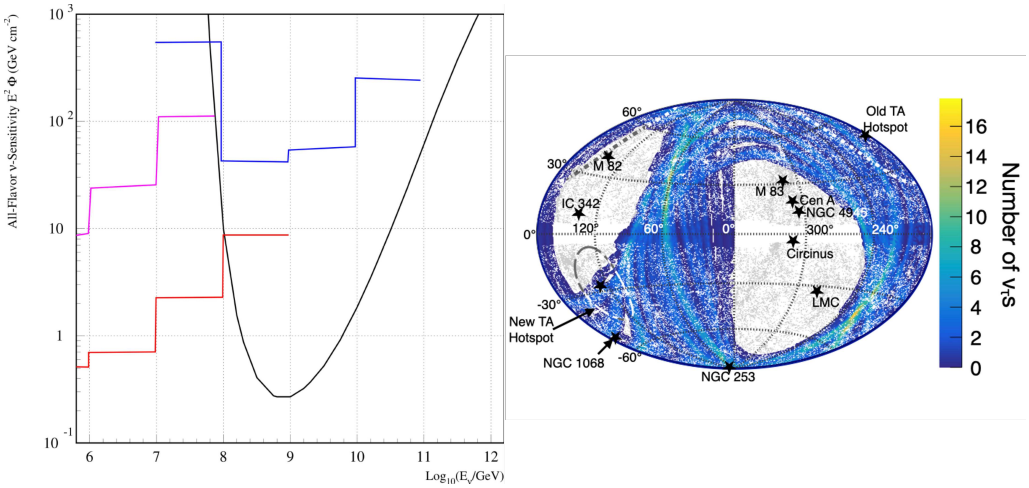

Figure 8. (**Left**): Optimal 1000 s sensitivity for an April 2023 flight (black), compared with Auger (blue), IceCube (red), and ANTARES (magenta) limits for GW170817 [15]. (**Right**): PBR's 100-day average number of ν_τ events as a function of source location, assuming a BNS merger model [14] at 3 Mpc distance. Black stars indicate nearby sources [15].

4. Conclusions

The next-generation stratospheric balloon mission under development by the JEM-EUSO collaboration is PBR, which represents a critical step toward enabling space-based observations of Ultra-High-Energy Cosmic Rays (UHECRs) and Very-High-Energy Neutrinos (VHENs). Building on the heritage of EUSO-SPB1 and EUSO-SPB2, PBR integrates a 1.1 m modified Schmidt optical system together with the first sub-orbital implementation of a hybrid, POEMMA-inspired focal surface, thereby advancing the technological maturity required for future space missions. PBR will provide the first direct measurement of fluorescence emission from UHECR-induced extensive air showers from above the atmosphere. In addition, it will conduct dedicated observations of high-altitude horizontal air showers. It will perform searches for upward-going events induced by Earth-skimming neutrinos, particularly during Target-of-Opportunity (ToO) follow-up observations triggered by astrophysical alerts. These measurements will help refine detection strategies and constrain models of UHECR acceleration and propagation [29]. A distinctive advancement of PBR is the inclusion of a dual-polarized radio instrument capable of detecting coherent radio emission in the 60–660 MHz band. Operating in conjunction with the optical Cherenkov cameras, this system enables, for the first time, truly hybrid optical–radio observations of extensive air showers from a balloon platform. The combined measurement approach provides an independent validation channel, enhances event classification, and strengthens sensitivity to near-horizon and upward-going geometries. The mission is scheduled for launch in spring 2027 from Wanaka, New Zealand, as part of NASA's Super Pressure

Balloon program, with a planned duration exceeding 20 days. The stratospheric vantage point, wide tilting capability, and hybrid detection architecture of PBR will substantially expand the observable volume for UHECRs and VHENs, making the mission an essential precursor to a future space-based POEMMA-class observatory.

Author Contributions: Conceptualization, A.O., G.O. and J.E.; methodology, A.O., G.O. and J.E.; software, J.E.; validation, all; investigation, all; resources, A.O. and G.O.; writing—original draft preparation, G.O. and J.E.; writing—review and editing, G.O. and J.E.; visualization, G.O. and J.E.; supervision, A.O., G.O. and J.E.; project administration, A.O. and G.O.; funding acquisition, A.O. and G.O. All authors have read and agreed to the published version of the manuscript.

Funding: This research was funded by NASA awards 80NSSC22K1488 and 80NSSC24K1780, by the French space agency CNES, the Istituto Nazionale di Fisica Nucleare and the Italian Space agency ASI. The work is supported by OP JAC and financed by ESIF and the MEYS CZ.02.01.01/00/22_08/0004596.

Data Availability Statement: Dataset available upon request from the authors.

Acknowledgments: The authors would like to gratefully acknowledge the collaboration and expert advice provided by the PUEO collaboration. This research used resources of the National Energy Research Scientific Computing Center (NERSC), a U.S. Department of Energy Office of Science User Facility operated under Contract No. DE-AC02-05CH11231. We acknowledge the NASA Balloon Program Office, the Columbia Scientific Balloon Facility, the French space agency CNES, the Italian Space Agency ASI, and their staff for their support. We also acknowledge the invaluable contributions of the administrative and technical staff at our home institutions.

Conflicts of Interest: The authors declare no conflicts of interest.

Abbreviations

The following abbreviations are used in this manuscript:

MIZAR	Multi-Channel Integrated Zone-Sampling Analog-Memory-Based Readout
ASIC	Application Specific Integrated Circuit
POEMMA	Probe of Extreme Multi-Messenger Astrophysics
UHECR	Ultra-High Energy Cosmic Ray
SiPM	Silicon Photo-Multiplier
CN	Cosmic Neutrino
EAS	Extensive Air Shower
ADC	Analog-to-Digital Converter
FPGA	Field-Programmable Gate Array
CMOS	Complementary Metal–Oxide–Semiconductor
FE	Front-End
INFN	Istituto Nazionale di Fisica Nucleare
PBR	POEMMA–Balloon with Radio
JEM-EUSO	Joint Experiment Missions for Extreme Universe Space Observatory
EUSO-SPB2	Extreme Universe Space Observatory–Super Pressure Balloon 2
M-EUSO	Mini-Extreme Universe Space Observatory
MAPMT	Multi-Anode Photomultiplier Tube

References

1. The Pierre Auger Collaboration. The Pierre Auger Cosmic Ray Observatory. *Nucl. Instrum. Methods Phys. Res. A Accel. Spectrom. Detect. Assoc. Equip.* **2015**, *798*, 172–213. [CrossRef]
2. Kawai, H.; Yoshida, S.; Yoshii, H.; Tanaka, K.; Cohen, F.; Fukushima, M.; Hayashida, N.; Hiyama, K.; Ikeda, D.; Kido, E.; et al. Telescope array experiment. *Nucl. Phys. B Proc. Suppl.* **2008**, *175–176*, 221–226. [CrossRef]
3. Aartsen, M.G.; Ackermann, M.; Adams, J.; Aguilar, J.A.; Ahlers, M.; Ahrens, M.; Altmann, D.; Andeen, K.; Anderson, T.; Ansseau, G.; et al. The IceCube Neutrino Observatory: Instrumentation and Online Systems. *J. Instrum.* **2017**, *12*, 03012–03091. [CrossRef]

4. Tinyakov, P.; Anchordoqui, L.; Bister, T.; Biteau, J.; Caccianiga, L.; de Almeida, R.; Deligny, O.; di Matteo, A.; Giaccari, U.; Harari, D.; et al. The UHECR dipole and quadrupole in the latest data from the original Auger and TA surface detectors. In *Proceedings of the 37th International Cosmic Ray Conference PoS(ICRC2021)*; Sissa Medialab srl Partita IVA: Trieste, Italy, 2021; Volume 395, p. 375. [CrossRef]
5. Coleman, A.; Eser, J.; Mayotte, E.; Sarazin, F.; Schröder, F.G.; Soldin, D.; Venters, T.M.; Aloisio, R.; Alvarez-Muñiz, J.; Alves Batista, R.; et al. Ultra high energy cosmic rays: The intersection of the Cosmic and Energy Frontiers. *Astropart. Phys.* **2023**, *149*, 102819. [CrossRef]
6. Aab, A.; Abreu, P.; Aglietta, M.; Ahn, E.J.; Al Samarai, I.; Albuquerque, I.F.M.; Allekotte, I.; Allison, P.; Almela, A.; Alvarez Castillo, J.; et al. The Pierre Auger Observatory Upgrade—Preliminary Design Report. *arXiv* **2016**, arXiv:1604.03637. [CrossRef]
7. Kido, E. Status and prospects of the TAx4 experiment. *EPJ Web Conf.* **2019**, *210*, 6001–6003. [CrossRef]
8. Aartsen, M.G.; Ackermann, M.; Adams, J.; Aguilar, J.A.; Ahlers, M.; Ahrens, M.; Altmann, D.; Anderson, T.; Anton, G.; Arguelles, C.; et al. IceCube-Gen2: A Vision for the Future of Neutrino Astronomy in Antarctica. *arXiv* **2014**, arXiv:1412.5106. [CrossRef]
9. Horandel, J.R. The Global Cosmic Ray Observatory. In *Proceedings of the 37th International Cosmic Ray Conference PoS(ICRC2021)*; Sissa Medialab srl Partita IVA: Trieste, Italy, 2021; Volume 395, p. 027. [CrossRef]
10. Álvarez-Muñiz, J.; Batista, R.A.; Balagopal, A.V.; Bolmont, J.; Bustamante, M.; Carvalho, W., Jr.; Charrier, D.; Cognard, I.; Decoene, V.; Denton, P.B.; et al. The Giant Radio Array for Neutrino Detection (GRAND): Science and Design. *Sci. China Phys. Mech. Astron.* **2020**, *63*, 219501–219542. [CrossRef]
11. The POEMMA Collaboration; Olinto, A.V.; Krizmanic, J.; Adams, J.H.; Aloisio, R.; Anchordoqui, L.A.; Anzalone, A.; Bagheri, M.; Barghini, D.; Battisti, M.; et al. The POEMMA (Probe of Extreme Multi-Messenger Astrophysics) observatory. *J. Cosmol. Astropart. Phys.* **2021**, *2021*, 007. [CrossRef]
12. Plebaniak, Z. From Ground to Space: An Overview of the JEM-EUSO Program for the Study of UHECRs and Astrophysical Neutrinos. In *Proceedings of the 39th International Cosmic Ray Conference PoS(ICRC2025)*; Sissa Medialab srl Partita IVA: Trieste, Italy, 2025; Volume 501, p. 360. [CrossRef]
13. The JEM-EUSO Collaboration. EUSO-SPB1 mission and science. *Astropart. Phys.* **2024**, *154*, 102891. [CrossRef]
14. The JEM-EUSO Collaboration. The Extreme Universe Observatory on a Super-Pressure Balloon II: Mission, Payload and Flight. *arXiv* **2025**, arXiv:2505.20762. [CrossRef]
15. Eser, J.; Olinto, A.V.; Osteria, G. POEMMA-Balloon with Radio: An Overview. *PoS ICRC2025* **2025**, *249*, 1–10. [CrossRef]
16. Cafagna, F.S. The Fluorescence Camera for the PBR mission. In *Proceedings of 39th International Cosmic Ray Conference PoS(ICRC2025)*; Sissa Medialab srl Partita IVA: Trieste, Italy, 2025; Volume 501, p. 249. [CrossRef]
17. Scotti, V.; Anastasio, A.; Bertaina, M.; Boiano, A.; Caruso, R.; De Santis, C.; Masone, V.; Mese, M.; Osteria, G.; Panico, B.; et al. The Cherenkov Camera for the PBR mission. In *Proceedings of the 39th International Cosmic Ray Conference PoS(ICRC2025)*; Sissa Medialab srl Partita IVA: Trieste, Italy, 2025; Volume 501, p. 391. [CrossRef]
18. Bertaina, M.; Palmieri, P.A.; Bargelli, M.; Da Rocha Rolo, M.D.; Dellacasa, G.; Di Salvo, A.; Garbolino, S.; Mazza, G.; Mignone, M.; Rivetti, A.; et al. Performance results of the first version of the MIZAR ASIC for the PBR mission. *arXiv* **2025**, arXiv:2511.12273. [CrossRef]
19. Scotti, V.; Osteria, G.; Mese, M.; Anastasio, A.; Boiano, A.; Buckland, I.; Masone, V.; Munini, R.; Panico, B.; Qureshi, H.A.; et al. The SiSMUV Project: Development and Characterization of SiPM-Based UV-Light Detectors for Space Telescope Applications. *Particles* **2025**, *8*, 92. [CrossRef]
20. Abarr, Q.; Allison, P.; Ammerman Yebra, J.; Alvarez-Muñiz, J.; Beatty, J.; Besson, D.; Chen, Y.; Chen, C.; Xie, J.M.; Clem, A.; et al. The Payload for Ultrahigh Energy Observations (PUEO): A white paper. *J. Instrum.* **2021**, *16*, 8035–8073. [CrossRef]
21. Krizmanic, J.; Mitchell, J.; Cummings, A.L.; Garcia, F. Extensive Air Shower (EAS) Development in the Upper Atmosphere: A unique environment to measure the EAS properties. In *Proceedings of the 38th International Cosmic Ray Conference PoS(ICRC2023)*; Sissa Medialab srl Partita IVA: Trieste, Italy, 2023; Volume 444, p. 524. [CrossRef]
22. Abe, S.; Adams, J.H., Jr.; Allard, D.; Alldredge, P.; Aloisio, R.; Anchordoqui, L.; Anzalone, A.; Arnone, E.; Baret, B.; Barghini, D.; et al. EUSO-Offline: A comprehensive simulation and analysis framework. *J. Instrum.* **2024**, *19*, 1007–1027. [CrossRef]
23. The JEM-EUSO Collaboration. The EUSO-SPB2 fluorescence telescope for the detection of Ultra-High Energy Cosmic Rays. *Astropart. Phys.* **2025**, *165*, 103046–103060. [CrossRef]
24. Bergmann, T.; Engelm, R.; Heck, D.; Kalmykov, N.N.; Ostapchenko, S.; Pierog, T.; Thouw, T.; Werner, K. One-dimensional hybrid approach to extensive air shower simulation. *Astropart. Phys.* **2007**, *26*, 420–432. [CrossRef]
25. Pierog, T.; Karpenko, I.; Katzy, J.M.; Yatsenko, E.; Werner, K. Epos lhc: Test of collective hadronization with data measured at the CERN large hadron collider. *Phys. Rev. C* **2015**, *92*, 034906. [CrossRef]
26. Aab, A.; Abreu, P.; Aglietta, M.; Albury, J.M.; Allekotte, I.; Almela, A.; Alvarez Castillo, J.; Alvarez-Muñiz, J.; Alves Batista, R.; Anastasi, G.A.; et al. Measurement of the cosmic-ray energy spectrum above 2.5×10^{18} using the Pierre Auger Observatory. *Phys. Rev. D* **2020**, *102*, 062005. [CrossRef]

27. Cummings, A.L.; Aloisio, R.; Krizmanic, J.F. Modeling of the Tau and Muon Neutrino-induced Optical Cherenkov Signals from Upward-moving Extensive Air Showers. *Phys. Rev. D* **2021**, *103*, 043017. [CrossRef]
28. Cummings, A.L.; Aloisio, R.; Eser, J.; Krizmanic, J.F. Modeling the optical Cherenkov signals by cosmic ray extensive air showers directly observed from suborbital and orbital altitudes. *Phys. Rev. D* **2021**, *104*, 063029. [CrossRef]
29. Guépin, C.; Kotera, K.; Oikonomou, F. High-energy neutrino transients and the future of multi-messenger astronomy. *Nature Rev. Phys. D* **2022**, *4*, 697–712. [CrossRef]
30. Venters, T.M.; Reno, M.H.; Krizmanic, J.F.; Anchordoqui, L.A.; Guépin, C.; Olinto, A.V. POEMMA's Target of Opportunity Sensitivity to Cosmic Neutrino Transient Sources. *Phys. Rev. D* **2020**, *102*, 123013. [CrossRef]
31. Reno, M.H.; Krizmanic, J. νSpaceSim: A Comprehensive Simulation Package for Modeling the Measurement of Cosmic Neutrinos using the Earth as the Neutrino Target and Space-based Detectors. In *Proceedings of the 39th International Cosmic Ray Conference PoS(ICRC2025)*; Sissa Medialab srl Partita IVA: Trieste, Italy, 2025; Volume 501, p. 1082. [CrossRef]
32. Albert, A.; Andre, M.; Anghinolfi, M.; Ardid, M.; Aubert, J.-J.; Aublin, J.; Avgitas, T.; Baret, B.; Barrios-Marti, J.; Basa, S.; et al. Search for High-energy Neutrinos from Binary Neutron Star Merger GW170817 with ANTARES, IceCube, and the Pierre Auger Observatory. *Astrophys. J. Lett.* **2017**, *850*, 20650. [CrossRef]